Study of Nonpolar Solvation Dynamics in Supercritical Lennard−Jones Fluids in Terms of the Solvent Dynamic Structure Factor

Tsuyoshi Yamaguchi,*,† Yoshifumi Kimura,‡,§ and Masaru Nakahara†

Institute for Chemical Research, Kyoto University, Uji, Kyoto 611-0011, Japan, and Department of Chemistry, Graduate School of Science, Kyoto University, Kyoto 606-8502, Japan

Received: February 28, 2002; In Final Form: May 24, 2002

The nonpolar solvation dynamics in Lennard−Jones fluids is discussed in terms of the relationship with the dynamic structure factor of neat solvent, using the theoretical expression that describes the solvation correlation function as the superposition of solvent dynamic structure factors at various wavenumbers. Several expressions for the coupling strength between the state transition of the solute and the solvent density modes are examined with respect to their abilities to predict the static fluctuation. In the present theoretical model, it is found that the difference between the ground- and excited-state solute−solvent interactions can be adequately taken as the coupling strength with the solvent density mode. Employing this expression for the coupling, the solvent fluctuation around $k \cong \sigma^{-1}$ (σ stands for the diameter of the solvent) contributes dominantly to the static fluctuation in all the densities investigated. This corresponds to the feature of the solvation dynamics in mixed solvents, in which the effective wavenumber is determined to be $1.14\sigma^{-1}$ from the proportionality between the solvation rates and the diffusion coefficients in the higher-density region. The half decay time ($t_{1/2}$) of the dynamic structure factor at this wavenumber shows similar density dependence to that of the solvation correlation function obtained in our previous work. The half decay time of the dynamic structure factor is correlated with the static structure factor. This supports our previous proposal that the curvature of the free energy surface along the solvation coordinate is essential to the solvation dynamics. The agreement between the present theory and the simulation is further improved by taking the motion of the solute into account.

I. Introduction

Studies on the fluctuation and the relaxation of solvent molecules around a solute molecule are required for a deep understanding of chemical processes in solution. The dynamic aspects of solvent around the solute, called "solvation dynamics", can be accessed by monitoring the state transition of the solute by means of such optical methods as fluorescence dynamic Stokes shift, transient hole burning, and photon echo. The molecular level elucidation of these dynamic processes has long been a target of a variety of theoretical and computer simulation studies.[1−7]

Roughly speaking, the solvation dynamics can be divided into two categories, the polar (ionic or dipolar) and the nonpolar ones. Until now, much more attention has been paid to the former than to the latter. In the polar solvation dynamics, for example, the dipole moment of the solute molecule changes due to the state transition of the solute in polar solvents, and the relaxation of the solvent molecules is easily observed experimentally as a result of the large solvent reorganization energy. This process is important in connection with electron-transfer reactions and dielectric friction.[8,9] The nonpolar solvation dynamics, where the solute−solvent nonpolar interaction varies with the state transition of the solute, is studied less intensively than the polar solvation dynamics, although the former is also important to understand vibrational energy relaxation, solute diffusion, and other molecular processes in solution. Some computer simulations have focused on the nonpolar solvation dynamics,[4,5] and Berg et al. measured experimentally the solvation dynamics accompanied by the change of the solute−solvent repulsive interaction.[10] To our knowledge, however, there has been no experimental study on nonpolar solvation dynamics due to the change of the solute−solvent isotropic attractive interaction.

The attractive nonpolar solvation dynamics has not been observed under the ambient conditions for the following reason. In dense liquids under the ambient conditions, the solvent density around the solute can hardly respond to the change of the solute−solvent isotropic attractive interaction because the solvent molecules are closely packed in dense liquids. The repulsive interaction is dominant in the nonpolar solvation dynamics there. In low- and medium-density fluids, on the other hand, the solvation structure is very sensitive to the attractive interaction between solute and solvent.[11] The attractive nonpolar solvation dynamics is thus expected to play a significant role in chemical processes in the medium-density region of supercritical fluids. The number of experimental studies on the solvation dynamics in supercritical fluids is very small, probably due to experimental difficulties.[12] According to some computer simulations, the translational motion of solvents is responsible for the polar solvation in the low-density region, whereas the

* To whom correspondence should be addressed. Present address: Department of Molecular Design and Engineering, Graduate School of Engineering, Nagoya University, Chikusa, Nagoya, Aichi, 464-8603, Japan. E-mail: tyama@nuce.nagoya-u.ac.jp.

† Institute for Chemical Research.

‡ Department of Chemistry.

§ Present address: International Innovation Center, Kyoto University, Kyoto, 606-8501, Japan.

10.1021/jp0205719 CCC: $22.00 © 2002 American Chemical Society
Published on Web 08/08/2002

rotational motion of solvents causes the polar solvation dynamics in dense liquids.[13,14]

To investigate the problem, we have already performed a molecular dynamics (MD) simulation study on the nonpolar solvation dynamics in three-dimensional Lennard−Jones (LJ) fluids including gaslike, supercritical, and liquidlike densities.[15] The important points clarified in that paper are as follows. When the attractive part of the solute−solvent interaction is coupled to the state transition of the solute, the solvation time is almost independent of the solvent density at lower densities ($\rho\sigma^3 < 0.35$; ρ and σ stand for the number density and the molecular diameter, respectively), and it decreases with an increase in the solvent density in the higher-density region. It was also clarified that the static fluctuation of the solvent molecules within the attractive interaction region is much smaller than that expected from the compressibility of the bulk solvent; i.e., the local solvent fluctuation around the solute molecules is not described well by the bulk properties of the solvent. We have to include the local properties of the fluid to account for the nonpolar solvation dynamics in supercritical fluids. In our previous paper,[15] we have correlated the solvation time with the static local fluctuation of the solvent around the solute and discussed the correlation in terms of the curvature of the free energy surface along the solvation coordinate.

After our simulation study,[15] Maddox et al. performed the MD simulation on LJ fluids of lower dimensionality,[16] and calculated the time correlation function of the fluctuation of the local density around a tagged particle. Maddox et al. have also found that the relaxation time has a maximum around the critical density when the area of the local region becomes larger. From this result, they have argued that the slowing down of the long-range critical fluctuation is important for the relaxation of the local density fluctuation around a tagged particle. They have also found the small density dependence of the relaxation time from the low- to medium-density regions when the solvent density within the first solvation shell is probed, as was found in our previous work, because the properties treated are essentially similar.[15] They explained this small density dependence in terms of the competition between the critical slowing down and the activation process from the attractive well produced by the solute molecule.

One of the central issues in the study of solvation dynamics is to realize how the solvation dynamics and the properties of the neat solvent are related, although the solvation dynamics is dependent on the properties of the solute in principle. It is desirable to examine if the solvation dynamics can be realized essentially in terms of the properties of the neat solvent. In such a case, our knowledge on the solvation dynamics from the study on a particular model molecule can be extended to other systems of more chemical interest.

The continuum model of the solvent is one of the simplest approaches to understand the solvation dynamics from the properties of the bulk solvent. In this model, the solvent is approximated as a dielectric continuum, e.g., for the polar solvation dynamics.[17] Viscoelastic models are corresponding continuum models used for the nonpolar solvation dynamics, in which an isotropic part of the solute−solvent interaction is involved in the state transition of the solute.[18] Whereas only the macroscopic (long wavelength) properties of the solvent are used in the continuum model, the solvent properties on the molecular level are taken into account in microscopic theories. In this work, we will apply the microscopic model for the solvation dynamics to explain the simulation results on the nonpolar solvation dynamics in fluids from low- to high-density regions. We will try to identify what kind of solvent motion in the local field of the solute affects the solvation dynamics at the respective density. In this course, the difference between the interpretation of Maddox et al. and ours will be clarified by the comparison between the solvation dynamics and the solvent dynamic structure.

II. Models and Theoretical Methods

II.A. Model. The potential model employed in this work is the same as system 1 of our previous work.[15] In the ground state of the solute, both the solute−solvent and the solvent−solvent interactions are the Lennard−Jones 12-6 potential given by

$$v(r) = 4\epsilon\left\{\left(\frac{\sigma}{r}\right)^{12} - \left(\frac{\sigma}{r}\right)^{6}\right\} \tag{1}$$

where $v(r)$ stands for the intermolecular interaction in the ground state. The parameters ϵ and σ are the same for the solute (X) and the solvent (S). The mass of the solute is also the same as that of the solvent, which is denoted as m. The solute−solvent interaction increases by $u(r)$ on the excitation of the solute, and the solute−solvent interaction becomes $v(r) + u(r)$ in the excited state. As the explicit expression of $u(r)$, we use the attractive part of the LJ potential as follows,

$$u(r) = \begin{cases} -\epsilon & (r < 2^{1/6}\sigma) \\ 4\epsilon\left\{\left(\frac{\sigma}{r}\right)^{12} - \left(\frac{\sigma}{r}\right)^{6}\right\} & (r > 2^{1/6}\sigma) \end{cases} \tag{2}$$

Hereafter we use the reduced unit so that ϵ, σ, k_B (Boltzmann constant), and m are unity. The instantaneous transition energy shift due to the solvent, $\Delta U(t)$, is given as the sum of the contribution of each solvent molecule. This is expressed by

$$\Delta U(t) = \sum_{i \in S} u(r_{iX}) \tag{3}$$

where i is the index of molecules, and S and X stand for the solvent and the solute, respectively.

In our previous work,[15] we performed equilibrium MD simulations by keeping the solute in its ground state and calculated the time correlation function of $\delta\Delta U(t)$ ($=\Delta U(t) - \langle\Delta U(t)\rangle$). Thus, only the solvent dynamics under the ground-state solute−solvent interaction is probed in our model; i.e., we probe the solvation dynamics of the excited state under the linear response assumption, whereas the solvent dynamics on the excited-state potential surface can also be involved in some real experiments such as the fluorescence dynamic Stokes shift measurement. It is also to be noted that the difference in the solute−solvent interaction on the ground and the excited states of the solute is limited to the first solvation shell at most. Therefore, our model is essentially the same as one of the models of Maddox et al.[16] when the range of the local region, denoted r_l in their paper, is equal to 1.78. In fact, our model is equivalent to theirs when the square-well potential is chosen as $u(r)$, because $\Delta U(t)$ is proportional to the number of solvent molecules within the well in such a case.

II.B. Theoretical Basis. In most of microscopic theories on the solvation dynamics, the solvation correlation function is described as a superposition of the solvent dynamic structure factors or their molecular versions at different wavenumbers with the coupling parameter describing the solute−solvent interaction. In simple fluids, the solvation correlation function, which is an equilibrium time correlation function of the

transition energy of the solute, is expressed by the following equation:[6,7]

$$\langle \delta\Delta U(0)\, \delta\Delta U(t)\rangle = \frac{\rho}{2\pi^2}\int_0^\infty \mathrm{d}k\, k^2 |\tilde{\phi}(k)|^2 F(k,t) \qquad (4)$$

Here ρ, $\delta\Delta U(t)$, and $F(k,t)$ stand for the number density of the solvent, the transition energy of the solute at time t, and the dynamic structure factor of the solvent, respectively. $\tilde{\phi}(k)$ is the coupling parameter between the state transition of the solute and the solvent density field at the wavenumber k. The tilde means the Fourier transform with respect to the space; that is, $\tilde{\phi}(k)$ is the Fourier transform of the real-space function $\phi(r)$. There are several choices of the coupling parameter, $\phi(r)$, whose explicit expressions will be introduced later.[6,7] The correlation function in eq 4 is not normalized here, because the initial value is also of certain importance. In the case of molecular liquids, $\phi(r)$ and $F(k,t)$ have suffixes that represent the sites of the solute and the solvent.[7] This kind of theory has been applied to the polar solvation dynamics under ambient conditions and succeeded in explaining the experimental and the computer simulation results.

II.C. Choice of Coupling Parameter. In the previous subsection, we have introduced the expression for the solvation correlation function in terms of the solvent dynamic structure factor; see eq 4. In this expression, the solvation correlation function is described as the superposition of the solvent density fluctuations at different wavenumbers. There are several choices of the coupling strength, $\phi(r)$, as introduced below.

The simplest choice of the coupling strength is $u(r)$ itself; i.e.,

$$\phi(r) = u(r) \qquad (5)$$

This expression is exact when the solute is an immobile test particle that does not interact with the solvent, because the solute molecule does not perturb the equilibrium distribution and the relaxation of the local solvent density. Hereafter this is denoted as model I. As will be shown later, eq 5 can be derived from the surrogate theory and the random phase approximation (RPA).

The solute−solvent radial distribution function may be multiplied to $u(r)$. This is called model II and expressed as

$$\phi(r) = g_{\mathrm{SX}}(r)\, u(r) \qquad (6)$$

This expression can be derived under a superposition-like approximation. Equation 6 is suggested by Vikhrenko et al.[19] as the improvement of the theory for the vibrational energy relaxation proposed by Hill.[20]

The third model, denoted as model III, is the linearized surrogate theory. In the surrogate theory for the nonequilibrium solvation dynamics,[7] the response function ($\langle\Delta U(t)\rangle_{\mathrm{ne}}$) is described as a weighted integral of the dynamic structure factor, and the coupling parameter is the difference in the solute−solvent direct correlation function between the initial and the final states [$\Delta\tilde{c}(k)$] as

$$\langle \Delta U(t)\rangle_{\mathrm{ne}} \propto \int_0^\infty \mathrm{d}k\, k^2 |\Delta\tilde{c}(k)|^2 F(k,t) \qquad (7)$$

On the other hand, when the difference in the solute−solvent interactions between the ground and the excited states is small, the nonequilibrium response function is equivalent to the equilibrium solvation correlation function in the linear response theory as

$$\langle \Delta U(t)\rangle_{\mathrm{ne}} \propto \langle \delta\Delta U(0)\, \delta\Delta U(t)\rangle \qquad (8)$$

When the coupling between the state-transition of the solute and the solute−solvent interaction is small, we can linearize $\Delta\tilde{c}(k)$; i.e., the difference of the direct correlation functions can be replaced by the derivative of the direct correlation function with respect to the coupling between the state transition of the solute and the solute−solvent interaction. As a result, in the linearized surrogate model, the coupling strength $\phi(r)$ is given by the following equation:

$$\phi(r) = -k_{\mathrm{B}}T\frac{\partial}{\partial\epsilon_u} c_{\mathrm{SX}}(r;\epsilon_u)|_{\epsilon_u=0} \qquad (9)$$

where ϵ_u stands for the extent of the difference in the strength of the solute−solvent interactions between the ground and the excited states. That is to say, the solute−solvent interaction is expressed as $v(r) + \epsilon_u u(r)$. The solute is in the ground or excited state when ϵ_u is equal to 0 or 1, respectively. The intermediate values of ϵ_u are also considered hypothetically. $c_{\mathrm{SX}}(r;\epsilon_u)$ means the solute−solvent direct correlation function. The hydrodynamic theory for the vibrational energy relaxation in supercritical fluid proposed by Cherayil and Fayer[21] belongs to this model.

Because the derivative of the solute−solvent direct correlation function is difficult to obtain directly from the simulation, we should introduce further approximations to evaluate model III numerically. We employ three different approximations as follows. The first two approximations are based on the perturbation theory of liquids. What is required here is the change of the direct correlation function in response to the change of the solute−solvent attractive interaction, for which perturbation theories work excellently, especially in the high-density region.[22] The first one, hereafter called model III-1, is the random phase approximation (RPA).[22] In RPA, the change of the direct correlation function in response to the variation of the solute−solvent attractive interaction is proportional to the attractive interaction itself. This leads to the expression as

$$\frac{\partial}{\partial\epsilon_u} c_{\mathrm{SX}}(r;\epsilon_u) = -\frac{1}{k_{\mathrm{B}}T} u(r) \qquad (10)$$

The substitution of eq 10 into eq 9 gives the same result as model I; see eq 5.

The second approximation, model III-2, is the LIN approximation.[22] In the LIN approximation, the derivative of the direct correlation function is given by the following rather complicated expression:

$$\frac{\partial}{\partial\epsilon_u} c_{\mathrm{SX}}(r;\epsilon)|_{\epsilon_u=0} = -\mathrm{FT}\left[\frac{1}{S(k)}\mathrm{FT}\left[g_{\mathrm{SX}}(r)\mathrm{FT}\left[S(k)\mathrm{FT}\left[\frac{u(r)}{k_{\mathrm{B}}T}\right]\right]\right]\right] \qquad (11)$$

where FT stands for the Fourier transform and $S(k)$ is the structure factor of the solvent. This expression follows from the relationship of the LIN approximation given by

$$\frac{\partial}{\partial\epsilon_u} h_{\mathrm{SX}}(r;\epsilon)|_{\epsilon_u=0} = -g_{\mathrm{SX}}(r)\mathrm{FT}\left[S(k)\mathrm{FT}\left[\frac{u(r)}{k_{\mathrm{B}}T}\right]\right] \qquad (12)$$

In addition to the approximations based on the perturbation theory, the direct numerical differentiation can be also performed; this is denoted as model III-3. In this model, the derivative of the direct correlation function is approximated to be the difference in the direct correlation functions between the neat solvent and the attractive solute as

$$\frac{\partial}{\partial \epsilon_u} c_{SX}(r;\epsilon_u)|_{\epsilon_u=0} = c_{SX}(r;\epsilon_u=1) - c_{SX}(r;\epsilon_u=0) \quad (13)$$

II.D. Details of Simulation. The quantities required to evaluate the right-hand side (rhs) of eq 4 were obtained from MD simulations. The equilibrium NVT simulations were performed by the Nosé−Hoover method. The temperature was kept at 1.5 and the density was varied from 0.10 to 0.95, as in the case of the previous simulation.[15] The simulation cell was composed of 500 particles. The direct correlation functions $c(r)$ and the static structure factors $S(k)$ were obtained by extending the radial distribution function using the method proposed by Verlet.[23,24] The dynamic structure factors $F(k,t)$ were evaluated from k_{min} to $32k_{min}$ at the interval of k_{min}, where k_{min} is equal to $2\pi(\rho/500)^{1/3}$. The radial distribution functions at $\epsilon_u = 1$ were taken from the previous simulation.[25]

III. Results and Discussions

We will discuss the solvation time in the nonpolar solvation dynamics due to the short-ranged attractive potential in terms of eq 4 in the following ways. First, in section III.A, we will mention the static fluctuation that is the initial value of the time correlation function. In this section, a proper model and the effective wavenumber contributing to the fluctuation are selected. Second, in the next section, the dynamics structure factor of the solvent, which determines the time profile in eq 4, is discussed. The characteristic value that determines the initial decay of the structure factor at the effective wavenumber is considered. In section III.C, by coupling the results in the previous two sections, the solvation time is considered in terms of eq 4. Finally, the critical anomaly will be discussed in section III.D.

III.A. Static Fluctuation. As mentioned above, several models are introduced for the strength of the coupling of the state transition of the solute with the density mode of the solvent. In this subsection, we evaluate the static fluctuation, i.e., the initial value of the correlation function, by these models. In this way, we can clarify the wavenumber region that is effectively operating in the static fluctuation.

Before the evaluation of the static solvation fluctuation, we show in Figure 1 the density dependence of the static structure factor obtained from the MD simulation. We calculate the static structure factor in two ways. First, the density field at each simulation step is Fourier transformed and its correlation function is evaluated. Second, the radial distribution function is obtained in the real space, and it is Fourier transformed by the method of Verlet.[23,24] The structure factors obtained from these two ways agree fairly well with each other, and we use that from the radial distribution function in the following calculations. The structure factor at the low wavenumber is large in the low- and medium-density regions, reflecting the long wavelength critical fluctuation. On the other hand, in the high-density region, the fluctuation at the low wavenumber is small, and the peak around $2\pi\sigma^{-1}$ grows with density.

The expression for the static fluctuation is derived by substituting $t = 0$ into eq 4 as follows:

$$\langle|\delta\Delta U|^2\rangle = \frac{\rho}{2\pi^2}\int_0^\infty \mathrm{d}k\, k^2|\tilde{\phi}(k)|^2 S(k) \quad (14)$$

The values of $\langle|\delta\Delta U|^2\rangle$ with different models for ϕ are plotted against the solvent density in Figure 2. The values of our previous simulation are also shown together. Surprisingly enough, the simplest model, model I (or model III-1) is the best among those considered here. We consider it is probably because RPA works well in the system considered here. Models II and III-2 cannot predict the decrease of the static fluctuation in the high-density region.

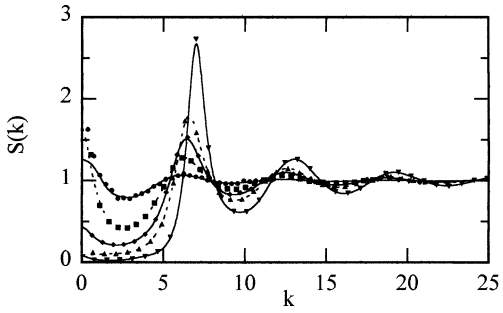

Figure 1. Static structure factor at various densities. Symbols and lines are those directly obtained from simulations and those evaluated from the radial distribution functions, respectively: (●) $\rho = 0.10$; (■) $\rho = 0.30$; (◆) $\rho = 0.55$; (▲) $\rho = 0.70$; (▼) $\rho = 0.95$. Please note that all the figures are described in the LJ reduced units.

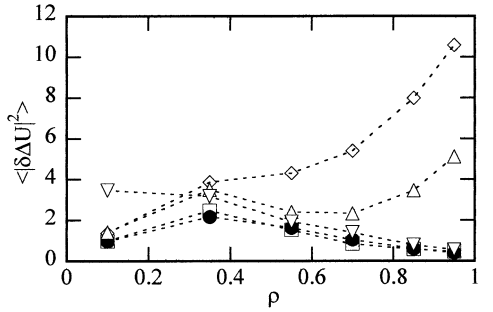

Figure 2. Static fluctuation of the transition energy, ($\langle|\delta\Delta U|^2\rangle$): (●) MD simulation (ref 15); (□) model I (or model III-1); (◇) model II; (△) model III-2; (▽) model III-3.

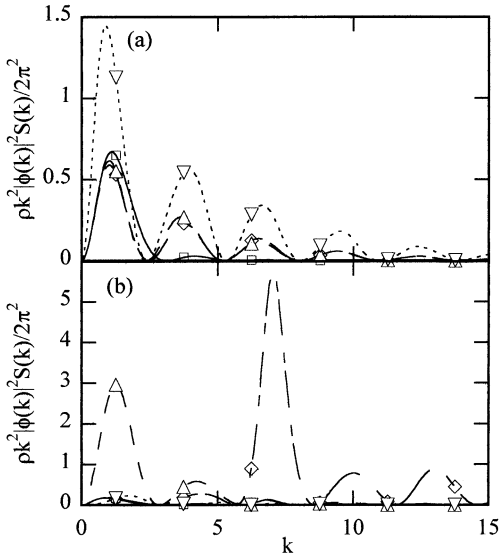

Figure 3. Integrands of the right-hand side of eq 14 of various models: (a) $\rho = 0.10$; (b) $\rho = 0.95$. Key: solid line with □, model I; dash-dotted line with ◇, model II; broken line with △, model III-2; dotted line with ▽, model III-3.

The integrands of eq 14 at $\rho = 0.10$ and 0.95 are plotted against the wavenumber in Figure 3 to analyze the differences between models in detail. It corresponds to the weighing function $I(k)$ in ref 6a. In the case of model II, the increase in the fluctuation comes from the wavenumber around the maximum of the static structure factor. Therefore, we consider that the small solvent motion around the repulsive core of the solute

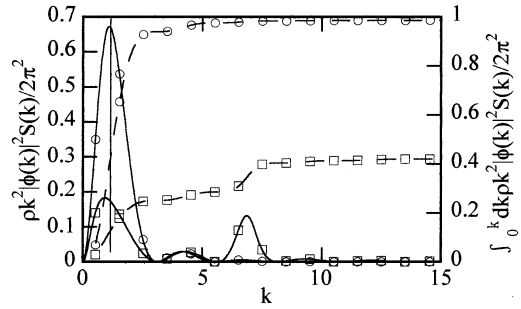

Figure 4. Integrand of the right-hand side of eq 14 with model I (solid lines). The circle and the square are those of $\rho = 0.10$ and $\rho = 0.95$. The integrands are integrated from 0 to k, and they are shown by the broken lines. The vertical line is the effective wavenumber from the nonpolar solvation dynamics in mixed solvent, which is explained in the text.

is the reason for the discrepancy of model II. Although the solvent motion near the repulsive core does not alter $u(r)$, it can induce a large change in $g(r)\,u(r)$, which is the reason for the overestimate of the static fluctuation of model II. On the other hand, model III-2 predicts that the fluctuation at the lower wavenumber ($k \sim 1$) is larger than those of other models, the reason of which we cannot understand at present. The values of model III-3 agree well with those of the simulation in the higher-density region, whereas they are not so good in the lower-density region. We consider that it is because of the nonlinearly of $c_{SX}(r;\epsilon_u)$ as a function of ϵ_u. We use model I in the latter part of this paper, because it describes the static fluctuation best among the models examined in this work.

The integration from 0 to k is also plotted together with the integrant in Figure 4 for model I. In the case of $\rho = 0.10$, the static fluctuation comes exclusively (about 90%) from the mode around $k \sim 1$. At $\rho = 0.95$, the mode around the maximum of the static structure factor ($k \sim 7$) also contributes to the static fluctuation, reflecting the decrease and the increase in $S(k)$ around $k \sim 1$ and $k \sim 7$, respectively. However, more than half of the fluctuation comes from $k \sim 1$ even at $\rho = 0.95$. Therefore, the solvent fluctuation around $k \sim 1$ is probed by the solvation dynamics in the model of our interest. The effective wavenumber is smaller than that of Bagchi[6a] because the repulsive part is not included in $u(r)$ of our model. The long-wavenumber mode involves motions of large numbers of molecules, which improves the linearity of the mode due to the central limiting theorem. We consider it is the reason for the good performance of the RPA. The wavenumber effective to the static fluctuation, of course, depends on the shape of $u(r)$. We can probe the fluctuation at lower wavenumber by employing $u(r)$ of a longer interaction range.

In the previous work, we performed the simulation of nonpolar solvation dynamics in mixed solvents and found that the solvation time is inversely proportional to the self-diffusion coefficient of the solvent in the high-density region.[15] Utilizing this proportionality, we can determine the wavenumber effective to the nonpolar solvation dynamics in mixed solvents by the following relationship:

$$t_{solv}^{-1} = 2Dk_{eff}^{2} \tag{15}$$

where t_{solv} and k_{eff} are the integrated solvation time and the effective wavenumber, respectively. The factor $2D$ is the interdiffusion coefficient between solute and solvent, which are the same kind of molecules in the model of ref 15. The value of k_{eff} is evaluated to be 1.14, which is shown as a vertical line in Figure 4. The value of k_{eff} determined dynamically is

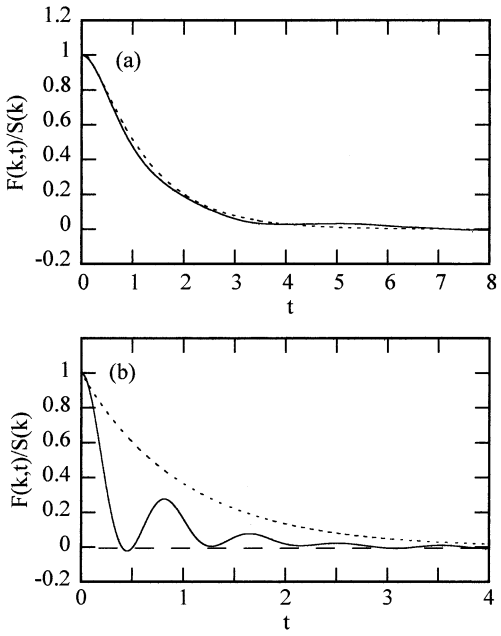

Figure 5. Time dependence of the dynamic structure factor: (a) $\rho = 0.35$ and $k = 1.12$; (b) $\rho = 0.95$ and $k = 0.78$. Solid and dotted curves are those from MD simulation and from eq 16, respectively.

consistent with the wavenumber-resolved fluctuation from eq 14, which justifies our determination of k_{eff}.

III.B. Dynamic Structure Factor. The time development of the solvation correlation function is determined by that of the solvent dynamic structure factor in our theory, eq 4. In this section, we will present how the relaxation of the solvent dynamic structure factor changes with solvent density. In Figure 5, we show the time dependence of the dynamic structure factor at representative densities and wavemunbers, $\rho = 0.35$ and $k = 1.12$ in Figure 5a, and $\rho = 0.95$ and $k = 0.78$ in Figure 5b. We have chosen these values of the wavenumber so that it can be close to k_{eff} determined in the previous subsection. The dotted curves in Figure 5 are the prediction from the single particle motion given by

$$F(k,t) = S(k)\exp\left[-\frac{k^2\delta r^2(t)}{6S(k)}\right] \tag{16}$$

where $\delta r^2(t)$ is the mean square displacement. Equation 16 gives the correct frequency moments up to the second order, and it reduces to the result of the Smolkovski−Vlasov equation,

$$F(k,t) = S(k)\exp\left[-\frac{Dk^2t}{S(k)}\right] \tag{17}$$

in the diffusive limit. Although eq 16 reproduces the dynamic structure factor at the medium-density well, it fails in the high-density region. The dynamic structure factor in the high-density region shows the viscoelastic behavior around k_{eff} due to the conservation of momentum density, contrary to the diffusive decay predicted by eq 16. It is consistent with our previous results that the diffusion-based models failed in the nonpolar solvation dynamics caused by the attractive interaction.

To clarify the relationship between the static structure factor and the short-time behavior of the dynamic structure factor, we plot $t_{1/2}$ together with $\sqrt{S(k)}/k$ in Figure 6. The densities of the fluid are 0.35 and 0.95 for Figure 4a,b, respectively. The ordinate axis is scaled so that they may agree with each other in the ideal gas limit. They therefore have to agree in the high-

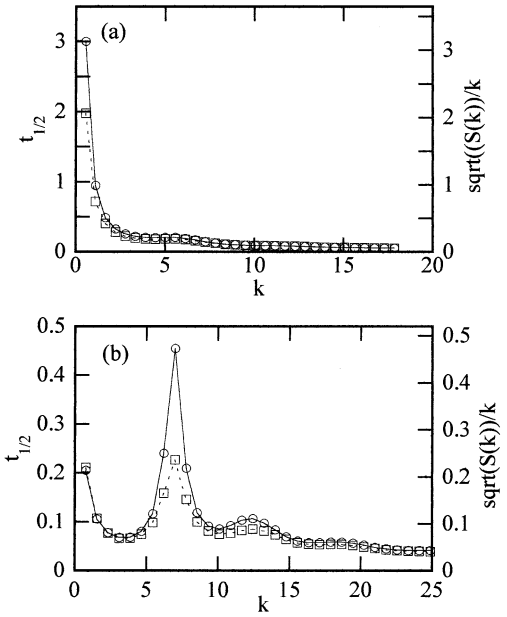

Figure 6. (Solid curves) half decay time of the dynamic structure factor and (dotted curves) $\sqrt{S(k)}/k$: (a) $\rho = 0.35$; (b) $\rho = 0.95$.

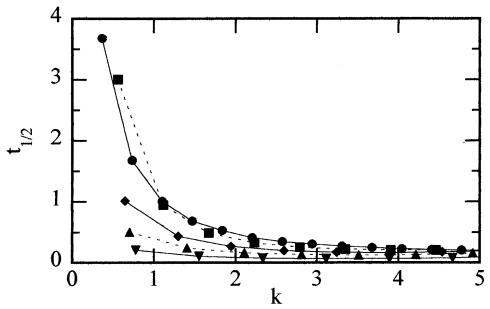

Figure 7. Half decay time of the dynamic structure factor at various wavenumbers: (●) $\rho = 0.10$; (■) $\rho = 0.30$; (◆) $\rho = 0.55$; (▲) $\rho = 0.70$; (▼) $\rho = 0.95$.

wavenumber limit at any density because the dynamic structure factor converges to that of the ideal gas in the high-wavenumber limit. As can be seen from Figure 6, the agreement of both values is satisfactory even in the lower wavenumber region, although some deviations are found at the large and slow mode ($k < 2$ at $\rho = 0.35$ and $k \sim 2\pi$ at $\rho = 0.95$). Because the value of $S(k)$ is the curvature of the free energy surface for the density fluctuation at k, the correlation between $\sqrt{S(k)}/k$ and $t_{1/2}$ means that the relaxation of the fluctuation is mainly dominated by the curvature of the free energy surface. In particular, the large static fluctuation of the low-wavenumber mode near the critical density is the principal reason for the slow relaxation of this mode, just as de Gennes' narrowing is induced by the large value of $S(k)$ around $k \sim 2\pi\sigma^{-1}$. The short-time part of $F(k,t)$ is naturally correlated to $S(k)$ because the second derivative of $F(k,t)/S(k)$ is inversely proportional to $S(k)$ exactly,[22,26] and the deviation in Figure 6 for the large and slow mode from $\sqrt{S(k)}/k$ is probably due to the deviation from the short time behavior.

The values of $t_{1/2}$ at various densities are plotted against wavenumber in Figure 7. The decay of the dynamic structure factor is slow in the low- and medium-density regions, corresponding to the large static density fluctuation, as shown in Figure 1. In our previous work, the density dependence of the solvation time is correlated with the normalized static fluctuation, $\langle|\delta\Delta U|^2\rangle/\langle-\Delta U\rangle$.[15] We have discussed this correlation in terms of the relationship between the short-time dynamics and the curvature of the free energy surface along the solvation coordinate. Based on eq 4, the static fluctuation and the solvation time are related to $S(k)$ and the relaxation time of $F(k,t)$, respectively. Thus, the correlation between $S(k)$ and $t_{1/2}$ of $F(k,t)$ is in harmony with our previous discussion.

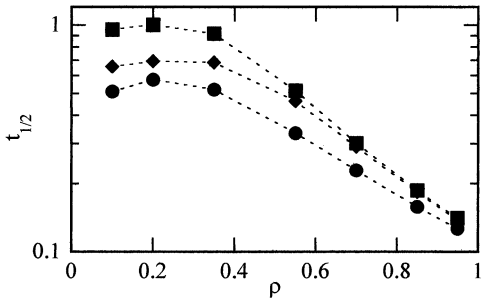

Figure 8. Half decay time of the solvation correlation functions: (●) MD simulation (ref 15); (■) eq 4; (◆) eq 18.

III.C. Solvation Time Viewed from the Dynamic Structure Factor. In Figure 8, the half decay time ($t_{1/2}$) of the solvation correlation function is compared with that of the dynamic structure factor at $k_{\text{eff}} = 1.14$. The value of $t_{1/2}$ at k_{eff} is obtained through the interpolation of the values $t_{1/2}$ at wavenumbers evaluated directly by the simulation. Although the direct evaluation of eq 4 is desirable, it is difficult due to the sparse sampling in the wavenumber space. Although we tried the direct integration of eq 4 with the sparse k-space sampling, the resulting solvation correlation function is not reliable quantitatively in that its initial value deviates from that in Figure 2 by 20% at $\rho = 0.95$.

The value of $t_{1/2}$ at k_{eff} is almost independent of the solvent density in the low-density region ($\rho < 0.35$), and it decreases with a decrease in the solvent density in the higher-density region. The overall trend of the density dependence is similar to that of the solvation correlation function, although the $t_{1/2}$ value of the dynamic structure factor is larger than that of the solvation correlation function. The discrepancy is larger at the lower density. This discrepancy is partially explained by the motion of the solute, as will be explained later.

The plateau in the low-density region is associated with the value of $k_{\text{eff}} = 1.14$ in this model. Because the range of $u(r)$ determines the value of k_{eff}, the fluctuation at lower wavenumber can be probed by lengthening the range of $u(r)$. In such a case, the value of $t_{1/2}$ of the solvation correlation function is expected to have a maximum value around the critical density due to the critical density fluctuation at long wavelengths. The maximum of the relaxation time around the critical density is actually observed by the MD simulation of 2D LJ fluid,[16] and our idea does not contradict with their explanation that the long wavelength critical density fluctuation is more important to the "local" density within the larger cutoff length.

The solute is as mobile as the solvent in this model, because the solute and solvent are of the same kind of molecule. The motion of the solute may therefore contribute to the solvation dynamics, which is neglected in eq 4. The motion of the solute can be included by replacing $F(k,t)$ in eq 4 with $F(k,t)\,F^s(k,t)$ as follows:[6b]

$$\langle\delta\Delta U(0)\,\delta\Delta U(t)\rangle = \frac{\rho}{2\pi^2}\int_0^\infty \mathrm{d}k\, k^2|\tilde{\phi}(k)|^2 F(k,t)\,F^s(k,t) \quad (18)$$

where $F^s(k,t)$ stands for the self-part of the dynamic structure factor of the solute. This equation resembles well the mode-coupling expression for the memory function of the self-

diffusion.[22,26,27] The above equation can be derived under the approximation that the density fields of the solute and the solvent follow the Gaussian process. The derivation is described in Appendix.

The $t_{1/2}$ value of $F(k,t)\,F^s(k,t)$ is plotted in Figure 8 together with those of solvation correlation function and $F(k,t)$. The agreement is improved in the low-density region by using $F(k,t)\,F^s(k,t)$ instead of $F(k,t)$. There still remains some discrepancy between the model and the simulation. It may be because we have used the $t_{1/2}$ value at a single wavenumber, whereas the solvation correlation function is expressed as the superposition of the contribution at various wavenumbers in eqs 4 and 18. This approximation can get worse especially in the higher-density region, because the contribution of the wavenumber around the peak of the structure factor to the static fluctuation is substantial. The solvation dynamics is expected to become slower in the supercompressed region, where the slow dynamics characteristic to the supercooled liquid develops. As is well-known, the slow dynamics of supercooled liquids stems from the density fluctuation around the peak of the structure factor,[28] and its contribution is necessary to reproduce the slow solvation dynamics in the supercompressed region. However, we consider that the effect of the supercompressed slow dynamics is small in the density region investigated here and that the agreement is satisfactory in view of the simplicity of the model.

In this work, we have mainly focused on the short-time behavior of the solvation correlation function as represented by $t_{1/2}$. It is to be recalled that the solvation time is often defined as the time integration of the normalized solvation correlation function, which can be strongly affected by the long-time behavior of the solvation correlation function. However, $t_{1/2}$ and the integrated solvation time follow the similar density dependence in our previous simulation,[15] and we consider that our conclusion in this work also applies to the time-integrated solvation time.

III.D. In the Critical Region.[29] In this subsection, the nonpolar solvation dynamics around the critical point is discussed on the basis of eq 18. As shown in Appendix, eq 18 is derived under the assumption of the Gaussian process. According to the central limiting theorem, a variable is likely to follow the Gaussian statistics when the motions of many particles are involved there. Therefore, we consider that, although the short-time dynamics of liquids may not obey the Gaussian process,[30] the Gaussian approximation is likely to hold for the slow dynamics at the long wavenumber. This justifies our use of eq 18 near the critical point for the long wavelength fluctuation.

Provided that the collective fluctuation at the long wavelength relaxes much slower than the single-particle one in the critical region, we can neglect the time development of $F(k,t)$ in eq 18 to yield the following equation:

$$\langle \delta\Delta U(0)\,\delta\Delta U(t)\rangle = \frac{\rho}{2\pi^2}\int_0^\infty \mathrm{d}k\, k^2|\tilde{\phi}(k)|^2 S(k)\,F^s(k,t) \qquad (19)$$

The static structure factor, $S(k)$, is approximated by the Ornstein−Zernike formula,

$$S(k) = \frac{a\xi^2}{1+k^2\xi^2} \qquad (20)$$

where a is a constant and ξ stands for the correlation length. In this subsection, we consider only the contribution of the hydrodynamic wavenumber ($k \ll \sigma^{-1}$). As clearly seen in eq 18, the Ornstein−Zernike formula does not have the correct high-wavenumber limit, and it underestimates the fluctuation on the molecular scale; see Figure 1. Therefore, the use of the Ornstein−Zernike formula is not justified when one treats the phenomena that probe the fluctuation in the high-wavenumber region, such as the vibrational energy relaxation.

The self-part of the dynamic structure factor is approximated to be purely diffusive,

$$F^s(k,t) = \exp(-Dk^2t) \qquad (21)$$

where D means the self-diffusion coefficient of the solute. We neglect the critical anomaly of the self-diffusion coefficient, because it is quite small if any.[31,32]

Equations 20 and 21 are substituted into eq 19 to get the final expression as follows:

$$\langle \delta\Delta U(0)\,\delta\Delta U(t)\rangle \cong \frac{a\rho}{2\pi^2}\int_0^\infty \mathrm{d}k\,\frac{k^2\xi^2|\tilde{\phi}(0)|^2\exp[-Dk^2t]}{1+k^2\xi^2} \qquad (22)$$

The wavenumber dependence of $\tilde{\phi}(k)$ is neglected in eq 22.

The initial value of the time correlation function (static fluctuation) is given by substituting $t = 0$ into eq 22,

$$\langle|\delta\Delta U|^2\rangle \cong \frac{a\rho}{2\pi^2}\int_0^\infty \mathrm{d}k\,\frac{k^2\xi^2|\tilde{\phi}(0)|^2}{1+k^2\xi^2} \qquad (23)$$

The integrand of eq 23 is finite in the critical limit ($\xi \to \infty$), which means that the critical density fluctuation does not lead to the divergence of the static solvent fluctuation felt by a solute. It is consistent with the discussion in our previous work that the fluctuation of ΔU should be finite because ΔU has both the upper and lower limits.

The critical limit of eq 23 is given by the following equation:

$$\langle \delta\Delta U(0)\,\delta\Delta U(t)\rangle \to \frac{a\rho}{2\pi^2}\int_0^\infty \mathrm{d}k\,|\tilde{\phi}(0)|^2\exp[-Dk^2t]$$

$$= \frac{a\rho|\tilde{\phi}(0)|^2}{4\pi\sqrt{\pi Dt}} \qquad (24)$$

Therefore, the solvation correlation function should decay to zero even in the critical limit. Exactly speaking,

$$\forall\epsilon > 0, \quad \forall\xi > 0, \quad \exists t, \quad |\langle \delta\Delta U(0)\,\delta\Delta U(t)\rangle| < \epsilon \qquad (25)$$

In particular, it is to be noted that the value of $t_{1/2}$ exhibits no critical anomaly. In contrast, the integrated value of the time correlation function diverges in the critical limit. It would require an extra treatment of the system size effect, however, to demonstrate the divergent behavior due to the power law decay that originates from the long-wavelength fluctuation.[33]

The above discussions have been concerned with the system in which the value of $\tilde{\phi}(0)$ is not zero. There however exist the cases that $\tilde{\phi}(0)$ is equal to zero. The mode-coupling expression of the memory function for the self-diffusion is such an example, where $\tilde{\phi}(k)$ is proportional to $k\tilde{c}(k)$.[27] In this case, the critical limit of the solvation correlation function obeys the $t^{-3/2}$ decay, and the integrated value of the correlation function is finite. This is consistent with our neglect of the critical anomaly of the self-diffusion coefficient.

IV. Summary

In this work, the nonpolar solvation dynamics in the LJ fluid is discussed in relation with the dynamic structure factor. After

the expression for the solvation correlation function is given in terms of the dynamic structure factor, several models for the coupling strength between the state transition of the solute and the solvent density are tested in the evaluation of the static fluctuation of the transition energy. The static fluctuation is described well by the theory if we treat the change of the solute−solvent interaction on the state transition of the solute as the coupling strength between the transition of the solute and the solvent density. The solvent density fluctuation around $k_{\mathrm{eff}} = 1.14\sigma^{-1}$ is probed in our model, which is consistent with the solvation time in the mixed solvent.

The half decay time ($t_{1/2}$) of the solvation correlation function and that of the dynamic structure factor at k_{eff} are shown to have quite similar density dependence, and their agreement is improved by taking the motion of the solute into account. This indicates that the nonpolar solvation dynamics in supercritical fluids is described well by the dynamic structure factor of the neat solvent and that the solvent fluctuation *within the local region* is the principal factor in the density dependence of the solvation time. The half decay time of the dynamic structure factor is correlated well with the static structure factor, as shown in Figure 6, which is explained in terms of the curvature of the free energy surface. Therefore, the slow relaxation of the local solvent fluctuation is ascribed to the large static fluctuation of the solvent density within the local region around the solute in the medium-density region. In particular, we could explain qualitatively our simulation result without extra mechanisms such as the activation process.

Acknowledgment. This work is supported by the Grant-in-Aid for Creative Scientific Research (13NP0201) from the Ministry of Education, Culture, Sports, Science, and Technology and by the Grant-in-Aid for Scientific Research (13440179) from JSPS. T.Y. acknowledges a research fellowship from the Japan Society of the Promotion of Science (JSPS) for Young Scientists.

Appendix: Derivation of Eq 18

From eq 4 the instantaneous transition energy shift is given by the product of the solvent and solute density modes as follows:

$$\begin{aligned}\Delta U(t) &= \sum_{i\in S} u(r_{iX}(t)) \\ &= \int\int \mathrm{d}\mathbf{r}_1\, \mathrm{d}\mathbf{r}_2\, u(\mathbf{r}_{12})\, \rho_S(\mathbf{r}_1,t)\, \rho_X(\mathbf{r}_2,t) \\ &= \sum_{\mathbf{k}} \tilde{\rho}_S(\mathbf{k},t)\, \tilde{\rho}_X(-\mathbf{k},t)\, \tilde{u}(\mathbf{k}) \qquad \text{(A-1)}\end{aligned}$$

where ρ_S and ρ_X stand for the density of the solute and solvent, respectively. The infinite dilution limit of the solute is assumed here. Hence, the time correlation function of $\delta\Delta U$ is given by the following equation:

$$\begin{aligned}&\langle \delta\Delta U(0)\, \delta\Delta U(t)\rangle = \\ &\sum_{\mathbf{k}_1,\mathbf{k}_2} \langle \tilde{\rho}_S(-\mathbf{k}_1,0)\, \tilde{\rho}_X(\mathbf{k}_1,0)\, \tilde{\rho}_S(\mathbf{k}_2,t)\, \tilde{\rho}_X(-\mathbf{k}_2,t)\rangle \tilde{u}(-\mathbf{k}_1)\, \tilde{u}(\mathbf{k}_2) \\ &\qquad - |\langle \sum_{\mathbf{k}} \tilde{\rho}_S(\mathbf{k},0) \tilde{\rho}_X(-\mathbf{k},0) \tilde{u}(\mathbf{k})\rangle|^2 \qquad \text{(A-2)}\end{aligned}$$

The four-point time correlation function in eq A-2 can be factorized into the product of two-point time correlation functions under the approximation that both ρ_S and ρ_X follow the Gaussian process as follows:

$$\begin{aligned}&\langle \tilde{\rho}_S(-\mathbf{k}_1,0)\, \tilde{\rho}_X(\mathbf{k}_1,0)\, \tilde{\rho}_S(\mathbf{k}_2,t)\, \tilde{\rho}_X(-\mathbf{k}_2,t)\rangle \\ &= \langle \tilde{\rho}_S(-\mathbf{k}_1,0)\, \tilde{\rho}_S(\mathbf{k}_2,t)\rangle\langle \tilde{\rho}_X(\mathbf{k}_1,0)\, \tilde{\rho}_X(-\mathbf{k}_2,t)\rangle \\ &+ \langle \tilde{\rho}_S(-\mathbf{k}_1,0)\, \tilde{\rho}_X(\mathbf{k}_1,0)\rangle\langle \tilde{\rho}_S(\mathbf{k}_2,t)\, \tilde{\rho}_X(-\mathbf{k}_2,t)\rangle \\ &+ \langle \tilde{\rho}_S(-\mathbf{k}_1,0)\, \tilde{\rho}_X(-\mathbf{k}_2,t)\rangle\langle \tilde{\rho}_X(\mathbf{k}_1,0)\, \tilde{\rho}_S(\mathbf{k}_2,t)\rangle \\ &= \langle \tilde{\rho}_S(-\mathbf{k}_1,0)\, \tilde{\rho}_S(\mathbf{k}_1,t)\rangle\langle \tilde{\rho}_X(\mathbf{k}_1,0)\, \tilde{\rho}_X(-\mathbf{k}_1,t)\rangle\delta_{\mathbf{k}_1,\mathbf{k}_2} \\ &+ \langle \tilde{\rho}_S(-\mathbf{k}_1,0)\, \tilde{\rho}_X(\mathbf{k}_1,0)\rangle\langle \tilde{\rho}_S(\mathbf{k}_2,t)\, \tilde{\rho}_X(-\mathbf{k}_2,t)\rangle \\ &+ \langle \tilde{\rho}_S(-\mathbf{k}_1,0)\, \tilde{\rho}_X(-\mathbf{k}_1,t)\rangle\langle \tilde{\rho}_X(\mathbf{k}_1,0)\, \tilde{\rho}_S(\mathbf{k}_1,t)\rangle\delta_{\mathbf{k}_1,\mathbf{k}_2} \qquad \text{(A-3)}\end{aligned}$$

The second term of eq A-3 cancels with the second term of eq A-2. In the infinite dilution limit, the first term is $O(N)$ (N stands for the number of solvent molecules), whereas the third one is $O(1)$, so that the latter is negligible. From the definition of the dynamic structure factor, the first term can be described as follows:

$$\begin{aligned}&\langle \tilde{\rho}_S(-\mathbf{k}_1,0)\, \tilde{\rho}_S(\mathbf{k}_1,t)\rangle\langle \tilde{\rho}_X(\mathbf{k}_1,0)\, \tilde{\rho}_X(-\mathbf{k}_1,t)\rangle\delta_{\mathbf{k}_1,\mathbf{k}_2} = \\ &\qquad NF(k_1,t)\, F^s(k_1,t)\delta_{\mathbf{k}_1,\mathbf{k}_2} \qquad \text{(A-4)}\end{aligned}$$

Equations A-3 and A-4 are substituted into eq A-2,

$$\begin{aligned}\langle \delta\Delta U(0)\, \delta\Delta U(t)\rangle &= N\sum_{\mathbf{k}_1,\mathbf{k}_2} F(\mathbf{k},t)\, F^s(\mathbf{k},t)|\tilde{u}(\mathbf{k}_2)|^2 \\ &= \frac{\rho}{2\pi^2}\int_0^\infty \mathrm{d}k\, k^2 F(k,t)\, F^s(k,t)|\tilde{u}(k)|^2 \qquad \text{(A-5)}\end{aligned}$$

The summation is replaced by the integral in the second line, and the isotropy of the liquid is used. The replacement of u by ϕ leads to the final expression, eq 18.

References and Notes

(1) Bagchi, B. *Annu. Rev. Chem. Phys.* **1989**, *40*, 115, and references therein.
(2) Maroncelli, M. *J. Mol. Liq.* **1993**, *57*, 1 and references therein.
(3) Stratt, R. M.; Maroncelli, M. *J. Phys. Chem.* **1996**, *100*, 12981 and references therein.
(4) Walsh, A. M.; Loring, R. F. *Chem. Phys. Lett.* **1991**, *186*, 77.
(5) (a) Saven, J. G.; Skinner, J. L. *J. Chem. Phys.* **1993**, *99*, 4391. (b) Stephens, M. D.; Saven, J. G.; Skinner, J. L. *J. Chem. Phys.* **1997**, *106* 1997. (c) Egorov, S. A.; Stephens, M. D.; Skinner, J. L. *J. Chem. Phys.* **1997**, *107*, 10485.
(6) (a) Bagchi, B. *J. Chem. Phys.* **1994**, *100*, 6658. (b) Biswas, R.; Bhattacharya, S.; Bagchi, B. *J. Chem. Phys.* **1998**, *108*, 4963.
(7) (a) Raineri, F. O.; Resat, H.; Perng, B.-C.; Hirata, F.; Friedman, H. L. *J. Chem. Phys.* **1994**, *100*, 1477. (b) Raineri, F. O.; Perng, B.-C.; Friedman, H. L. *Chem. Phys.* **1994**, *183*, 187. (c) Friedman, H. L.; Raineri, F. O.; Hirata, F.; Perng, B.-C. *J. Stat. Phys.* **1995**, *79*, 239.
(8) van der Zwan, G.; Hynes, J. T. *J. Phys. Chem.* **1985**, *89*, 4181.
(9) (a) Horng, M.-L.; Gardecki, J. A.; Maroncelli, M. *J. Phys. Chem. A* **1997**, *101*, 1030. (b) Maroncelli, M. *J. Chem. Phys.* **1997**, *106*, 1545.
(10) Ma, J.; Bout, D. V.; Berg, M. *J. Chem. Phys.* **1995**, *103*, 9146.
(11) See, e.g.: Kajimoto, O. *Chem. Rev.* **1999**, *99*, 355 and references therein.
(12) Kimura, Y.; Hirota, N. *J. Chem. Phys.* **1999**, *111*, 5457.
(13) Graf, P.; Nitzan, A. *Chem. Phys.* **1998**, *235*, 297.
(14) Re, M.; Laria, D. *J. Phys. Chem. B* **1997**, *101*, 10494.
(15) Yamaguchi, T.; Kimura, Y.; Hirota, N. *J. Chem. Phys.* **1999**, *111*, 4169.
(16) Maddox, M. W.; Goodyear, G.; Tucker, S. C. *J. Phys. Chem. B* **2000**, *104*, 6266.
(17) Hsu, C.-P.; Song, Xueyu, and Marcus, R. A. *J. Phys. Chem. B* **1997**, *101*, 2546.
(18) Berg, M. *J. Phys. Chem. A* **1998**, *102*, 17.
(19) Vikhrenko, V. S.; Schwarzer, D.; Schroeder, J. *Phys. Chem. Chem. Phys.* **2001**, *3*, 1000.
(20) Hills, B. P. *Mol. Phys.* **1978**, *35*, 1471.

(21) (a) Cherayil, B. J.; Fayer, M. D. *J. Chem. Phys.* **1997**, *107*, 7642. (b) Myers, D. J.; Shigeiwa, M.; Fayer, M. D.; Cherayil, B. J. *J. Phys. Chem. B* **2000**, *104*, 2402.

(22) Hansen, J. P.; McDonald, I. R.; *Theory of Simple Liquids*, 2nd ed.; Academic Press: London, 1986.

(23) Verlet, L. *Phys. Rev.* **1968**, *165*, 201.

(24) Allen, M. P.; Tildesley, D. J. *Computer Simulation of Liquids*; Oxford University Press: New York; 1987.

(25) Yamaguchi, T.; Kimura, Y. *Mol. Phys.* **2000**, *98*, 1553.

(26) Boon, J. P.; Yip, S. *Molecular Hydrodynamics*; McGraw-Hill: New York, 1980.

(27) (a) Sjögren, L.; Sjölander, A. *J. Phys. C* **1979**, *12*, 4369. (b) Sjögren, L. *J. Phys. C* **1980**, *13*, 705.

(28) Götze, W. *Liquids, Freezing and Glass Transition*; Elsevier: Amsterdam, 1991; Chapter 5.

(29) The infinitely dilute solution is considered throughout this work, although the infinite dilution limit is not commutable with the critical limit. In the discussion in section III-D, the infinite dilution limit is taken first and the critical limit is taken afterward.

(30) (a) Yamaguchi, T. *J. Chem. Phys.* **2000**, *112*, 8530. (b) Yamaguchi, T.; Kimura, Y. *J. Chem. Phys.* **2001**, *114*, 3029.

(31) Krynicki, K.; Meragi, A.-L.; Powles, J. G. *Ber. Bunsen-Ges. Phys. Chem.* **1981**, *85*, 1153.

(32) Kataoka, Y.; Fujita, M. *Bull. Chem. Soc. Jpn*, **1995**, *68*, 152.

(33) Erpenbeck, J. J.; Wood, W. W. *Phys. Rev. A* **1991**, *43*, 4254.